JOURNAL OF VIROLOGY, Jan. 2004, p. 266–274 Vol. 78, No. 1
0022-538X/04/$08.00+0 DOI: 10.1128/JVI.78.1.266–274.2004

Physical and Functional Interactions between Vaccinia Virus F10 Protein Kinase and Virion Assembly Proteins A30 and G7

Patricia Szajner,[1,2] Andrea S. Weisberg,[1] and Bernard Moss[1]*

Laboratory of Viral Diseases, National Institute of Allergy and Infectious Diseases, National Institutes of Health, Bethesda, Maryland 20892,[1] and Graduate Program of the Department of Genetics, The George Washington University, Washington, D.C. 20052[2]

Received 16 July 2003/Accepted 12 September 2003

An early step in vaccinia virus morphogenesis, the association of crescent membranes with electron-dense granular material, is perturbed when expression of the viral protein encoded by the A30L or G7L open reading frame is repressed. Under these conditions, we found that phosphorylation of the A17 membrane protein, which is mediated by the F10 kinase, was severely reduced. Furthermore, A30 and G7 stimulated F10-dependent phosphorylation of A17 in the absence of other viral late proteins. Evidence for physical interactions between A30, G7, and F10 was obtained by their coimmunoprecipitation with antibody against A30 or F10. In addition, phosphorylation of A30 was dependent on the F10 kinase and autophosphorylation of F10 was stimulated by A30 and G7. Nevertheless, the association of A30, G7, and F10 occurred even with mutated, catalytically inactive forms of F10. Just as A30 and G7 are mutually dependent on each other for stability, F10 was nearly undetectable in the absence of A30 and G7. The reverse is not true, however, as repression of F10 did not diminish A30 or G7. Interaction of F10 with A30 and G7 presumably occurred within the virus factory areas of the cytoplasm, where each was concentrated. F10 localized predominantly in the cortical region of immature virions, beneath the membrane where A17 is located. F10 remained associated with the particulate core fraction of mature virions after treatment with a nonionic detergent and reducing agent. The formation of protein complexes such as the one involving A30, G7, and F10 may be a mechanism for the regulated packaging and processing of virion components.

The assembly of vaccinia virus (VV), the prototype poxvirus, occurs within cytoplasmic viral factory areas that appear largely cleared of cellular organelles. Although studied intensively by electron microscopy, little is known about the molecular events involved in viral morphogenesis. Several viral proteins required for early stages of virus assembly have been identified through the characterization of temperature-sensitive and inducible conditional lethal mutants. Few recognizable membrane structures can be discerned in cells infected under nonpermissive conditions with mutants that map to the F10L open reading frame (ORF) (14, 18, 20). The product of the F10L ORF has been characterized as a dual-specificity protein kinase that phosphorylates tyrosine as well as serine and threonine residues of target proteins (1, 3, 8, 20). Mutated forms of F10, with single amino acid substitutions in the active site, were unable to transcomplement an inducible conditional lethal F10 mutant, confirming the importance of phosphorylation in virion assembly (14). Studies with F10 conditional lethal mutants suggest that the membrane components A17 (1, 3) and A14 (1) are substrates of the kinase. A17 is needed for an early step in viral membrane formation (11, 21) and A14 is needed at a slightly later stage of assembly (12, 19). The precursor of mature A17 is phosphorylated at serine, threonine, and tyrosine residues (1, 3) and is cleaved within viral protease AGX consensus sites after amino acids 17 and 185 (1, 10, 17). The phosphorylation state of A17 is also regulated by a dual-specificity protein phosphatase, the product of the VV H1 gene (3, 7, 9).

The association of the viral crescent membranes with electron-dense material containing internal virion components requires proteins encoded by the A30L, G7L, and J1R ORFs (2, 13, 15, 16). When expression of any of these proteins is repressed, the cytoplasmic viral factory regions contain large numbers of crescent-shaped and circular membranes distinctly separated from masses of electron-dense material. During those previous investigations, we noted subtle differences in the electrophoretic patterns of metabolically labeled proteins synthesized in the absence of A30 expression. As reported here, this led us to demonstrate a defect in phosphorylation of the A17 protein and an unanticipated association of the F10 kinase with a complex containing A30 and G7.

MATERIALS AND METHODS

ORF designations. ORFs are designated by a capital letter indicating a *Hin*dIII restriction endonuclease fragment, a number indicating the position in the *Hin*dIII fragment, and a letter (L or R) indicating the direction of transcription, e.g., F10L. The corresponding protein is designated by a capital letter and number, e.g., F10.

Cells and viruses. BS-C-1 (ATCC CCL6) and HeLa S3 (ATCC CCL2.2) cells were grown in Eagle's minimal essential medium (Quality Biologicals) and Dulbecco's modified eagle's medium (Quality Biologicals) supplemented with 10% fetal bovine serum (FBS), respectively. Unmodified VV (WR strain) and the recombinants vT7LacOI and vTF7-3 were propagated in HeLa cells as previously described (4). Recombinant vWT-F10V5 was propagated in HeLa S3 cells in the presence of 2.5% FBS; recombinant vA9i, vA30Li, vG7Li, vA17Li, vA30iHA-F10V5, and vF10V5i were grown in the continuous presence of 50 μM isopropyl-β-D-thiogalactopyranoside (IPTG) and 2.5% FBS. All virus stocks were stored at −70°C. Plaque assays and one-step virus growth experiments were carried out in BS-C-1 cells.

* Corresponding author. Mailing address: Laboratory of Viral Diseases, National Institutes of Health, 4 Center Dr., MSC 0445, Bethesda, MD 20892-0445. Phone: (301) 496-9869. Fax: (301) 480-1147. E-mail: bmoss@nih.gov.

Antibodies. Rabbit antipeptide sera against A30, A17, G7, and F10 were described previously (13, 14, 16, 21). The murine monoclonal antibody (MAb) MHA.11 conjugated to Alexa Fluor 488 was purchased from Covance Research Products Inc. (Denver, Pa.) and recognizes a nine-amino-acid influenza virus hemagglutinin (HA) epitope tag. Unconjugated and horseradish peroxidase-conjugated murine anti-V5 MAbs, which recognize the 14-amino-acid epitope of paramyxovirus simian virus 5, were purchased from Invitrogen (Carlsbad, Calif.). Anti-V5 antibody conjugated to agarose beads was from Sigma-Aldrich (St. Louis, Mo.). The rabbit polyclonal anti-phosphotyrosine (pTyr) and anti-phosphothreonine (pThr) antibodies and antibody inhibitors were from Zymed Laboratories (San Francisco, Calif.).

Plasmid construction. The plasmid used to replace the endogenous F10L ORF with a copy containing a V5 tag at the C terminus was derived from pSL1180GFPNeo, which encodes enhanced green fluorescent protein (GFP) under the control of the VV P11 promoter and the neomycin gene under the control of the VV P7.5 promoter. Part of the F10L ORF containing the V5 tag and the entire F9L ORF were separately amplified and sequentially cloned into the pSL1180GFPNeo plasmid. A fragment of 781 nucleotides, corresponding to the 3′ half of the F10L ORF, containing silent mutations at the 3′ end was generated by PCR using the VV genomic DNA as a template and the oligonucleotide primers 5′-GGATGGTCAGGAACTCTCATTGAG-3′ and 5′-CCAATTAGTTTCTTGGAAAAgTTcATcATGcGtGAtATaTTCagcGAtTGGATtAAcGGCGGgAAc-3′ (the mutated nucleotides are indicated with lowercase letters). Silent mutations were made in the 3′ end of the F10L ORF, which overlaps the F9 promoter, to prevent unwanted recombination of these sequences. To add the V5 tag to F10, the product of the first PCR was amplified by using the oligonucleotide primers 5′-GGATGGTCAGGAACTCTCATTGAG-3′ and 5′-TAAAGCGGCCGCTTA*CGTAGAATCGAGACCGAGGAGAGGGTTAGGGATAGGCTTACC*GTTCCCGCCGTTAATCCAATCG-3′ (the *Not*I site is underlined and the sequence of the V5 tag is in italics). This PCR product was digested with *Not*I and *Bst*BI restriction enzymes (the *Bst*BI site is within the F10L ORF) and cloned into pSL1180GFPNeo. A fragment containing the entire F9L ORF, including its promoter and flanked by *Not*I and *Xho*I sites, was generated by PCR using VV genomic DNA as a template and the oligonucleotide primers 5′-GCCGAATTGCGGCCGCAAAAATTTATTATGAGAGAC-3′ and 5′-CCGCTCGAGCATATGATGGCGGTGTACG-3′ (the *Not*I and *Xho*I sites are underlined). This PCR fragment was digested with *Not*I and *Xho*I restriction enzymes and cloned into pSL1180GFPNeo containing the V5-tagged copy of F10.

Western blotting. Western blotting of proteins from infected cell lysates or immunoprecipitated complexes was carried out as described previously (14). The membranes were incubated for 1 h with a 1:250 dilution of A30 antipeptide polyclonal antibody, a 1:5,000 dilution of anti-A17N polyclonal antibody or anti-V5 MAb, or a 1:1,000 dilution of anti-pTyr, anti-pThr, anti-G7, or anti-F10 polyclonal antibody. The membranes were washed in TTBS (100 mM Tris, pH 7.5, 150 mM NaCl, 0.1% [vol/vol] Tween 20) and incubated with either anti-rabbit or anti-mouse immunoglobulin G (IgG) conjugated to horseradish peroxidase (Amersham) at a 1:5,000 dilution. Bound IgG was detected by use of the SuperSignal West Pico chemiluminescent substrate (Pierce, Rockford, Ill.).

Metabolic labeling of proteins. BS-C-1 cells were infected with 10 PFU of virus per cell for 1 h at 37°C except where indicated. After adsorption, the cells were washed twice and incubated for 5 h with Eagle's minimal essential medium containing 2.5% FBS in the absence or presence of 50 μM IPTG. Six hours after infection, the medium was removed, replaced with methionine- and cysteine-free medium containing 2.5% dialyzed FBS (Invitrogen), and labeled with 50 μCi of [^{35}S]methionine and [^{35}S]cysteine per ml or 100 μCi of [^{32}P]orthophosphate per ml for an extra 18 h. The cells were then harvested, washed once with cold Tris-buffered saline, and subjected to immunoprecipitation as described below.

Immunoprecipitation analysis. Unlabeled or metabolically labeled cells were harvested 24 h after infection, washed with cold Tris-buffered saline, and incubated with lysis buffer (50 mM Tris [pH 8.0], 150 mM NaCl, 1% NP-40) in the presence of protease inhibitor cocktail tablets (Roche Molecular Biochemicals) for 30 min on ice. For detection of phosphorylated proteins, Na_3VO_4 and NaF were added to the lysis buffer to final concentrations of 0.2 and 50 mM, respectively. Lysates were clarified by centrifugation at 20,000 × *g* for 30 min at 4°C, rotated with 50 μl of 20% (vol/vol) protein A-Sepharose beads for 1 to 2 h at 4°C, and then centrifuged at 1,000 × *g* for 1 min. The supernatant was incubated overnight at 4°C with a 1:250 dilution of the anti-A30 (A30C) or anti-V5 antibody. Antigen-antibody complexes were then rotated with protein A-Sepharose beads for 1 to 2 h at 4°C. When using the anti-V5 and anti-HA antibodies conjugated to agarose beads, we incubated the cell lysates with the resin for 4 h at 4°C while rotating. The beads were washed four times with lysis buffer and resuspended in sample buffer (62.5 mM Tris-HCl [pH 6.8], 25% [vol/vol] glycerol, 2% (vol/vol) sodium dodecyl sulfate [SDS], 0.01% [vol/vol] bromophenol blue). Samples were incubated at 95°C for 3 min and analyzed by SDS-polyacrylamide gel electrophoresis (PAGE) and autoradiography.

Confocal microscopy. HeLa cells were grown to confluence on coverslips and infected with vA30iHA-F10V5 at a multiplicity of infection of 5 in the presence of 50 μM IPTG. After 12 to 18 h, cells were fixed with 4% paraformaldehyde and permeabilized with 0.1% Triton X-100, both in phosphate-buffered saline. The polyclonal anti-G7 antiserum was used at a 1:500 dilution followed by an anti-rabbit antibody conjugated to indodicarbocyanide (Cy5) (Jackson ImmunoResearch Laboratories, West Grove, Pa.) at a 1:100 dilution. The anti-V5 MAb was used at a 1:200 dilution followed by an anti-mouse antibody conjugated to rhodamine red X (Jackson ImmunoResearch Laboratories) at a 1:100 dilution. Anti-HA.11 MAb conjugated to Alexa Fluor 488 (Covance) was used at a 1:500 dilution. The coverslips were mounted in Mowiol containing 1 μg of 4′,6′-diamidino-2-phenylindole dihydrochloride (DAPI; Molecular Probes, Eugene, Oreg.) per ml to stain DNA. Images were collected on a Leica TCS-NT/SP inverted confocal microscope system and processed with Adobe Photoshop, version 6.0.

Immunoelectron microscopy. For immunoelectron microscopy, infected cells were fixed in a series of paraformaldehyde (Electron Microscopy Sciences, Fort Washington, Pa.) dilutions (2, 4, and 8% in 0.1 M phosphate buffer), washed in 0.1 M phosphate buffer, and incubated at 37°C in 10% gelatin. Samples were centrifuged and incubated on ice to solidify. The pellet was cut at 4°C into small cubes infiltrated with 2.3 M sucrose in 0.1 M phosphate buffer and frozen in liquid nitrogen. Ultracryosections were obtained by using the Leica Ultracut FCS microtome and were then placed on Formvar-carbon-coated grids. The sections were quenched with 0.02 M glycine in 0.1 M phosphate buffer, blocked with 0.1% fish skin gelatin in 0.01 M phosphate buffer (Sigma), and incubated with anti-V5 MAb at a 1:50 dilution. The sections were washed in 0.01% fish skin gelatin in 0.1 M phosphate buffer and incubated with a rabbit anti-mouse antibody followed by protein A conjugated to 10-nm-diameter colloidal gold (Department of Cell Biology, Utrecht University School of Medicine, Utrecht, The Netherlands). The sections were washed with 0.1% fish skin gelatin in 0.1 M phosphate buffer, followed by 0.1 M phosphate buffer and then deionized water. Samples were stained with uranyl acetate (Electron Microscopy Sciences) in methylcellulose (Sigma) and analyzed on the Philips CM100 transmission electron microscope.

Transient expression of A17, A30, G7, and F10. BS-C-1 cells in a six-well plate were infected with vTF7.3 (6) at a multiplicity of infection of 10 PFU per cell at 37°C in the absence or presence of 40 μg of cytosine arabinoside (AraC) per ml. After 1 h, the inocula were removed and the cells were washed three times with Opti-MEM I (Invitrogen), with or without 40 μg of AraC per ml. Cells infected with vTF7.3 in the presence of AraC were then transfected overnight with a total of 2 μg of plasmid in 10 μl of Lipofectamine 2000. Twenty-four hours after infection, cells were harvested and whole-cell lysates were prepared by the addition of sample buffer (62.5 mM Tris-HCl [pH 6.8], 25% [vol/vol] glycerol, 2% [vol/vol] SDS, 710 mM β-mercaptoethanol, 0.01% [vol/vol] bromophenol blue, 0.2 mM Na_3VO_4, and 50 mM NaF).

Virion subfractionation. VV particles, purified from infected cells by sedimentation through a sucrose cushion and gradient as previously described (5), were incubated in a reaction mixture containing 50 mM Tris-HCl (pH 7.5) and 1% (vol/vol) Nonidet P-40 (NP-40), with or without 50 mM dithiothreitol for 1 h at 37°C. The insoluble and soluble materials were separated by centrifugation at 20,000 × *g* for 30 min at 4°C. Proteins from the pellet and supernatant were analyzed by electrophoresis on a 4 to 20% gradient polyacrylamide gel in Tris-Tricine-SDS buffer (Invitrogen) followed by Western blotting.

RESULTS

Expression of A30 and G7 is required for tyrosine and threonine phosphorylation of A17. Upon SDS-PAGE, A17 appears as two incompletely resolved bands, with apparent masses of 23 to 25 kDa, and a well separated, faster migrating C-terminally truncated protein of 21 kDa. The VV conditional lethal mutants vA30Li and vG7Li (13, 16) were used to determine whether repression of A30 and G7 expression perturbed the processing of A17. The 23- to 25-kDa and 21-kDa A17 bands were detected upon SDS-PAGE of lysates of cells infected with vA30Li or vG7Li in the presence of inducer (Fig. 1). (Although the apparent masses of the A17 species were higher than previously reported, presumably due to different reference markers and gel conditions, we continued to use the

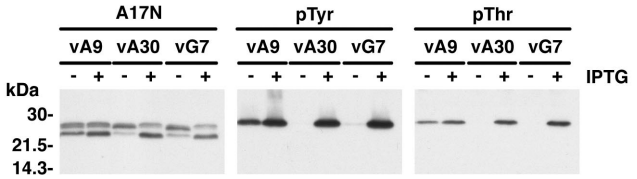

FIG. 1. A17 is not phosphorylated on tyrosine and threonine residues in the absence of A30 and G7 expression. (A) BS-C-1 cells were infected with vA9i (vA9), vA30Li (vA30), or vG7Li (vG7) virus in the presence (+) or absence (−) of 50 μM IPTG, as indicated. Twenty-four hours after infection, cells were harvested and total cell lysates were analyzed by electrophoresis in an SDS–4 to 20% gradient polyacrylamide gel in Tris-glycine buffer followed by Western blotting using the anti-A17N, anti-pTyr, and anti-pThr antisera. The migration positions and masses of marker proteins are indicated on the left.

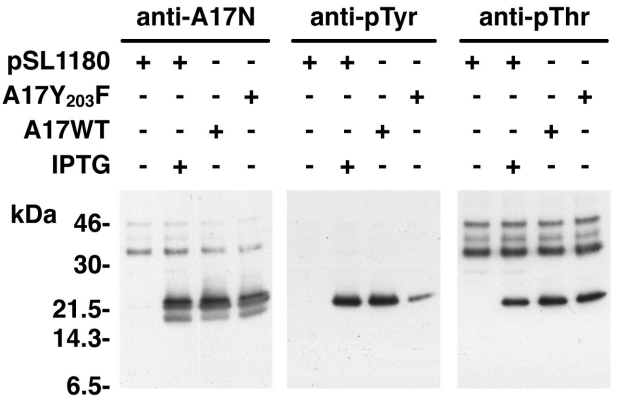

FIG. 2. Tyrosine and threonine phosphorylation of A17. BS-C-1 cells were infected with vA17Li at a multiplicity of infection of 5 PFU per cell in the presence (+) or absence (−) of 50 μM IPTG. Infected cells were transfected (+) with different combinations of plasmids containing a wild-type (A17WT) or mutated ($A17Y_{203}F$) form of the A17L ORF under the control of the P11 promoter or with vector alone (pSL1180), as indicated. At 24 h, cells were harvested and total cell lysates were analyzed by electrophoresis in an SDS–10 to 20% polyacrylamide gel in Tricine buffer followed by Western blotting using anti-pTyr, anti-pThr, or anti-A17N antiserum. Numbers on the left correspond to the molecular masses of marker proteins, in kilodaltons.

previous mass nomenclature for consistency.) In the absence of inducer, subtle differences in the A17 bands from cells infected with either vA30Li or vG7Li were noted. Only the lower of the incompletely resolved 23- to 25-kDa bands was detected and the band of 21-kDa was reduced in intensity and had a slightly slower mobility (Fig. 1). Because of these changes, the upper (23- to 25-kDa) and lower (21-kDa) A17 bands were closer to each other in the lanes containing proteins from the cells infected with vA30Li and vG7Li in the absence of IPTG than in the lanes containing proteins in its presence (Fig. 1, left panel). As a control, we also examined the A17 protein in cells infected with a conditional lethal VV mutant, vA9i, which requires IPTG for expression of the A9 membrane component. Under nonpermissive conditions, morphogenesis of vA9i is blocked between the immature virion and intracellular mature virion stages, but the viral membranes and viroplasm are not dissociated as occurs with A30 and G7 mutants (22). In cells infected with vA9i, the 23- to 25-kDa bands were similar under permissive and nonpermissive conditions, although the mobility of the 21-kDa species was slightly reduced in the absence of IPTG. These data suggested that formation of the 25-kDa species was specifically inhibited by repression of A30 or G7 expression.

A dramatic difference was observed when the effect of A30 or G7 repression on the phosphorylation state of A17 was analyzed. Both anti-pTyr and anti-pThr antibodies reacted with a 25-kDa band from cells infected with vA30Li or vG7Li in the presence of IPTG but not in its absence (Fig. 1, middle and right panels). Furthermore, the band recognized by the phosphorylation-specific antibodies corresponded precisely with the upper band detected with the A17N antibody, identifying the 25-kDa band as the phosphorylated A17 species. In contrast to the results obtained with vA30Li and vG7Li, repression of A9 had no significant effect on phosphorylation of A17, consistent with the detection of a 25-kDa band with A17N antiserum.

To confirm the identity of the band recognized by the anti-pTyr and anti-pThr antibodies, we infected cells with a recombinant VV that expresses A17 only in the presence of IPTG (21). As expected, the A17N antibody reacted with the 23- to 25-kDa and 21-kDa bands only when IPTG was present or when a plasmid expressing A17 was transfected (Fig. 2, left panel). Furthermore, pTyr and pThr antibodies reacted with a 25-kDa band only when the A17 protein was expressed (Fig. 2, middle and right panels). The A17N and pThr antibodies also reacted nonspecifically with some slower mobility proteins. In addition to a plasmid expressing wild-type A17, we also transfected one in which Tyr 203 was changed to Phe. Based on a report of Derrien and coworkers (3), we had anticipated that the anti-pThr antibody but not the anti-pTyr antibody would react with the mutated A17. Unexpectedly, this mutation reduced but did not prevent F10-dependent tyrosine phosphorylation of A17 (Fig. 2, middle panel). To resolve this discrepancy, we purchased pTyr antibody from the source (BD Transduction Laboratories, San Diego, Calif.) used by Derrien et al.. Using this other antibody, we also could not detect tyrosine phosphorylation of mutated A17 (data not shown). Therefore, the second pTyr antibody exhibits contextual sequence specificity, only recognizing phosphorylated tyrosine 203. However, there is at least one additional tyrosine residue in the A17 protein that is phosphorylated by the F10 kinase.

A30 dependence on A17 phosphorylation was not alleviated by a phosphatase inhibitor. Our inability to detect A17 from cells infected with vA30Li under nonpermissive conditions with anti-pTyr antibody could be explained either by reduced activity of the F10 kinase or by increased activity of the H1 phosphatase. To evaluate whether increased phosphatase activity was responsible for dephosphorylation of the tyrosine residues of A17, cells were infected with vA30Li in the presence or absence of IPTG and the nonspecific phosphatase inhibitor Na_3VO_4. As controls, cells were either mock infected or infected with vT7lacOI (the parent of the inducible viruses) in the presence or absence of Na_3VO_4. Whole-cell lysates were analyzed by SDS-PAGE followed by immunoblotting with anti-pTyr antibody. The addition of Na_3VO_4 caused an increase in the intensity of the 25-kDa band detected by the anti-pTyr antibody for the cells infected with vT7LacOI or with vA30Li in the presence of IPTG, consistent with inhibition of phos-

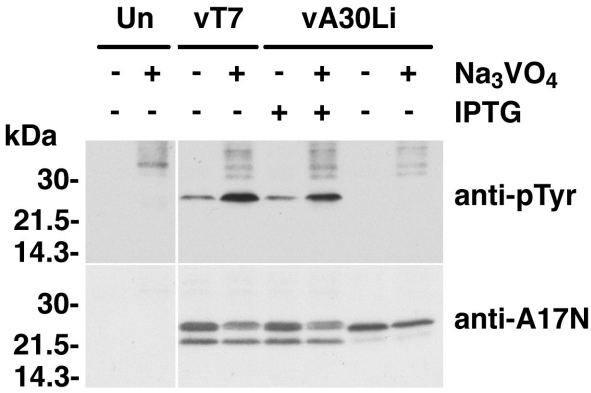

FIG. 3. Dependence of A17 phosphorylation on A30 and G7 was not circumvented by a phosphatase inhibitor. BS-C-1 cells were either mock infected (Un) or infected with vT7lacOI or vA30Li in the presence (+) or absence (−) of 50 μM IPTG. Four hours after infection, 100 μM Na_3VO_4 was added to the infected cells as indicated. Ten hours after infection, the cells were harvested and whole-cell lysates were analyzed by electrophoresis in an SDS–4 to 20% gradient polyacrylamide gel in Tris-glycine buffer followed by Western blotting using anti-pTyr or anti-A17N antibody, as indicated on the right. The migration positions and molecular masses of marker proteins are indicated on the left.

phatase activity (Fig. 3). Nevertheless, the addition of Na_3VO_4 did not relieve the inhibition of tyrosine phosphorylation of A17 in the cells infected with the vA30Li virus in the absence of IPTG (Fig. 3). The membrane used for the above experiment was stripped and reprobed with the anti-A17N serum to check whether addition of the phosphatase inhibitor had an effect on the expression or stability of A17. Although the 23- to 25-kDa doublet was slightly less intense in the presence of Na_3VO_4, the upper band seemed more prominent for the cells infected with vT7lacOI and vA30Li in the presence of IPTG, consistent with increased phosphorylation of A17 (Fig. 3). Taken together, these data suggested that the absence of tyrosine phosphorylation of A17 in cells infected with vA30Li in the absence of IPTG was caused by inhibition of F10 kinase activity rather than by increased activity of viral or cellular phosphatases.

Interaction of F10 kinase with G7 and A30. The failure of A17 to be phosphorylated by the F10 kinase when A30 or G7 expression was repressed could be explained by a spatial separation of the enzyme and substrate. Nevertheless, we decided to investigate the possibility of a more direct relationship between F10, A30, and G7. We previously showed that A30 and G7 interact with each other (13). To investigate a potential interaction of the G7 and A30 complex with F10, we made recombinant VVs containing the F10L ORF with a paramyxovirus simian virus 5 epitope tag at the C terminus. One of these, vF10V5i, with inducible expression of the F10V5 protein, is described in the accompanying paper (14). vWT-F10V5, another recombinant VV that expresses an epitope-tagged F10, was made by using wild-type VV as the parent. A third recombinant virus, vA30iHA-F10V5, was made starting with vA30iHA, in which the influenza virus HA tag was appended to the inducible A30L ORF, allowing the detection of the A30HA and F10V5 proteins simultaneously. Expression of the tagged proteins in cells infected with the recombinant VV was demonstrated by Western blotting and the proteins were functional, as gauged by the nearly normal size of plaques formed by the recombinant viruses under appropriate conditions (data not shown).

Extracts of cells infected with VV, vWT-F10V5, or vF10V5i in the presence or absence of IPTG were analyzed by Western blotting with anti-V5, anti-G7, and anti-A30 antibodies to confirm expression of the proteins. Similar levels of A30 and G7 were detected in the lysates of cells infected with the different viruses under permissive or nonpermissive conditions (Fig. 4A, left panel). As expected, V5-tagged F10 was present in lysates of cells infected with vWT-F10V5 and vF10V5i in the presence of IPTG but not in those of cells infected with wild-type VV WR or vF10V5i in the absence of IPTG (Fig. 4A, left panel). The same extracts were also incubated with the anti-V5 antibody, followed by protein A coupled to beads, and the bound proteins were analyzed by SDS-PAGE and immunoblotting. Bands corresponding to the G7 and A30 proteins were detected in the complex that was immunoprecipitated from cells infected with vWT-F10V5 or with vF10V5i in the presence of IPTG (Fig. 4A, right panel). These data provided evidence of a physical interaction between F10, A30, and G7.

In a variation of the above experiment, we infected cells with vF10V5i in the absence of IPTG and transfected the cells with plasmids expressing wild-type F10HA or F10HA with point mutations in the active site (14). Immunoprecipitation with HA antibody followed by Western blotting indicated that G7 interacted with catalytically inactive F10 as well as with the wild-type protein (data no shown).

The complex of F10, G7, and A30 was also demonstrated by use of an antibody against an epitope tag on A30. Cells were infected with vA30iHA-F10V5 in the presence of IPTG, and both the total lysate (Fig. 4B, left panel) and the HA MAb-bound complex (Fig. 4B, right panel) were analyzed. The presence of the three proteins in the complex was demonstrated by Western blotting (Fig. 4B). As a control, cells were infected with vWT-F10V5, in which the A30L ORF was not epitope tagged. In this case, the HA MAb did not coimmunoprecipitate the F10V5, G7, or A30 proteins (Fig. 4B).

Metabolic labeling provided additional information regarding the three proteins in the complex. Cells infected with VV WR, vWT-F10V5, or vA30iHA-F10V5 in the presence and absence of IPTG were labeled with [^{35}S]methionine and [^{35}S]cysteine. Cell extracts were incubated with the V5 antibody and immune complexes were analyzed by SDS-PAGE and autoradiography. A comparison of labeled complexes from cells infected with vWT-F10V5 and VV WR revealed 50-, 42-, and 9-kDa bands that were specific to the former virus (Fig. 4C). The 50-, 42-, and 9-kDa bands corresponded to F10V5, G7, and A30, respectively, as shown by analysis of proteins from cells infected with vA30Li and vG7Li in the presence and absence of IPTG (data not shown). In cells infected with the recombinant virus vA30iHA-F10V5, the 42-kDa protein coimmunoprecipitated with F10V5 for the cells infected in the presence but not the absence of IPTG (Fig. 4C), which is consistent with the fact that G7 does not accumulate in the absence of A30. In this experiment, A30HA was not resolved because the additional mass of the epitope tag caused it to comigrate with a background band. Although these experiments were not designed to determine the stoichiometry of the

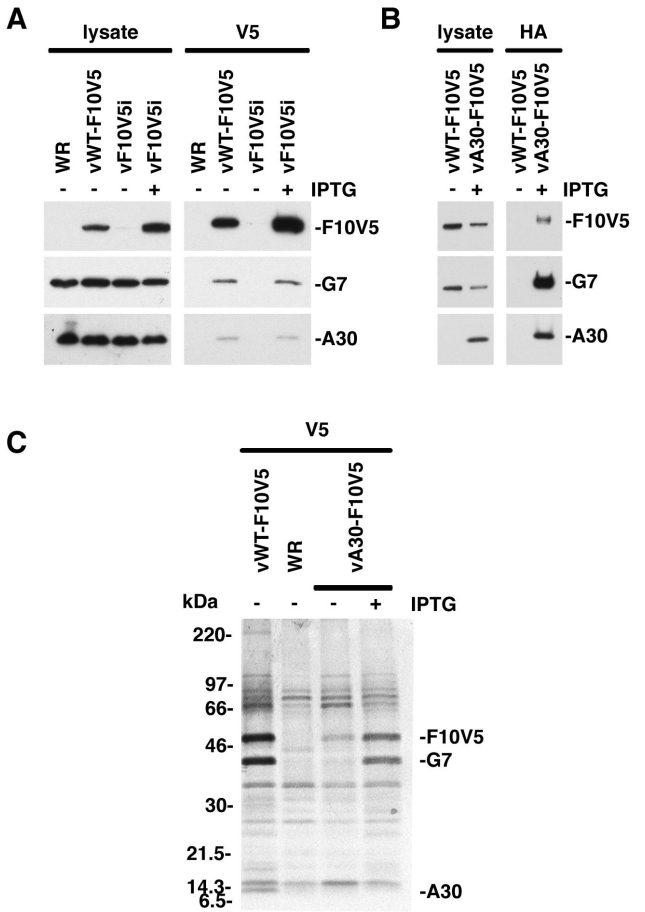

FIG. 4. Coimmunoprecipitation of G7 and A30 with F10V5 from infected cells. (A) BS-C-1 cells were infected with WT VV (WR), vWT-F10V5, or vF10V5i in the presence (+) or absence (−) of 50 μM IPTG, as indicated. Cells were harvested 24 h after infection and either whole-cell lysates or protein extracts were prepared. The extracts were incubated with the anti-V5 antibody conjugated to agarose beads. Both the antibody-bound proteins and the whole-cell lysates were analyzed by Western blotting using anti-G7 and anti-A30 antisera and the anti-V5 antibody conjugated with horseradish peroxidase. (B) BS-C-1 cells were infected with vWT-F10V5 or vA30iHA-F10V5 (vA30-F10V5) as indicated. Cells were harvested 24 h after infection and either whole-cell lysates or protein extracts were prepared. The extracts were incubated with the anti-HA antibody conjugated to agarose beads. Both the antibody-bound proteins and whole-cell lysates were analyzed by Western blotting using anti-G7 or anti-A30 antisera or anti-V5 antibody conjugated with horseradish peroxidase. The proteins were visualized by chemiluminescence. (C) BS-C-1 cells were infected with WT VV (WR), vWT-F10V5, or vA30iHA-F10V5 (vA30-F10V5) in the presence (+) or absence (−) of 50 μM IPTG, as indicated. Six hours after infection, the cells were incubated with a mixture of [^{35}S]methionine and [^{35}S]cysteine for 18 h at 37°C. Cell extracts were prepared and incubated with anti-V5 antibody. The antibody-bound products were resolved by SDS-PAGE and visualized by autoradiography. Bands corresponding to A30, G7, and F10V5 are indicated on the right. Numbers on the left correspond to molecular masses of the marker proteins.

complex, the relative intensities of the F10V5 and G7 bands suggest similar amounts of the two polypeptides. The low intensity of the A30 band is consistent with the presence of a single methionine and no cysteines.

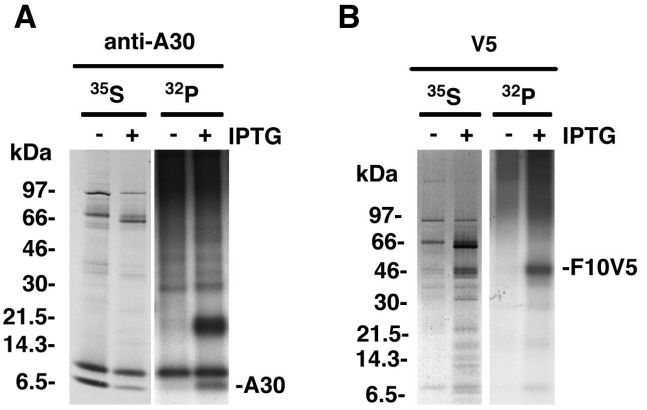

FIG. 5. Phosphorylation of A30 and F10V5. BS-C-1 cells were infected with vF10V5i in the presence (+) or absence (−) of IPTG and were metabolically labeled either with a mixture of [^{35}S]methionine and [^{35}S]cysteine (^{35}S) or with ^{32}Pi (^{32}P) for 18 h. Proteins were captured with anti-A30 (A) or anti-V5 (B) antibody. The antibody-bound proteins were resolved in an SDS–10 to 20% polyacrylamide gel in Tricine buffer and visualized by autoradiography. The bands corresponding to A30 and F10V5 are indicated on the right. The numbers on the left represent the molecular masses of marker proteins, in kilodaltons.

Although it is difficult to see in the reproduction (Fig. 4C), inspection of the ^{35}S-labeled protein complex revealed several additional weak bands that appear to have specifically coimmunoprecipitated with antibody against F10V5. Experiments are in progress to identify these proteins and determine the authenticity of their interactions with the complex.

F10-dependent phosphorylation of A30. The association of the F10 kinase with G7 and A30 raised the possibility that one or both of those proteins might be phosphorylated. To examine this, we infected cells with vF10V5i in the presence or absence of IPTG, metabolically labeled them with $^{32}P_i$ or [^{35}S]methionine and [^{35}S]cysteine, and incubated them with antibody. Cell lysis and washing of the antibody-bound proteins were carried out with a buffer containing SDS and deoxycholate, which is more stringent than the conditions used to preserve protein complexes. Analysis of ^{32}P-labeled proteins immunoprecipitated with the anti-A30 antibody revealed two bands specific for cells infected with vF10V5i in the presence of IPTG (Fig. 5A). The lower band corresponding to the A30 protein was also detected by labeling with ^{35}S, whereas the ^{32}P-labeled higher band was not significantly labeled with ^{35}S and may represent a highly phosphorylated viral or cellular component. ^{32}P- and ^{35}S-labeled bands corresponding in size to F10V5 were detected when anti-V5 MAb was used and cells were infected in the presence of IPTG (Fig. 5B). Autophosphorylation of purified F10 was reported previously (20).

F10 is unstable in the absence of A30 or G7 expression. We previously showed that A30 and G7 were each unstable in the absence of the other (13). To determine the stability of F10 in the absence of its partners, cells were infected with vA30Li or vG7Li in the presence or absence of IPTG. We also infected cells with vA9i, vA17Li, or vF10V5i in the presence or absence of IPTG to serve as controls. Whole-cell lysates were analyzed by SDS-PAGE followed by Western blotting with several different antibodies. The first row of Fig. 6 contains the relevant

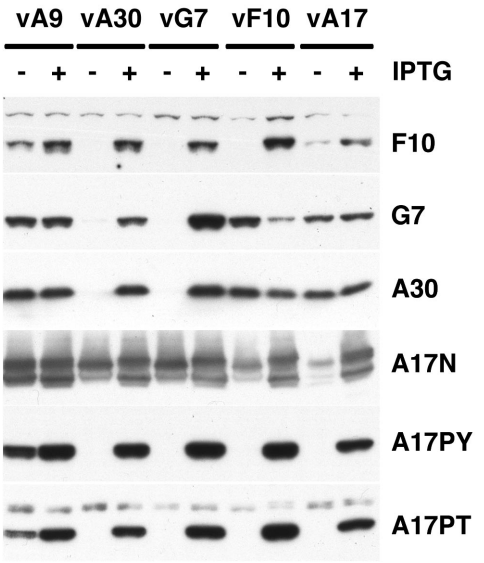

FIG. 6. Instability of F10 in the absence of A30 and G7 expression. BS-C-1 cells were infected with vA9i (vA9), vA30Li (vA30), vG7Li (vG7), vF10V5i (vF10), or vA17Li (vA17) in the presence (+) or absence (−) of IPTG, as indicated. Twenty-four hours after infection, cells were harvested and total cell lysates were analyzed by electrophoresis in an SDS–10 to 20% gradient polyacrylamide gel in Tricine buffer followed by Western blotting using anti-F10, anti-G7, anti-A30, anti-A17N, anti-pThr, and anti-pTyr antibodies, as indicated on the right.

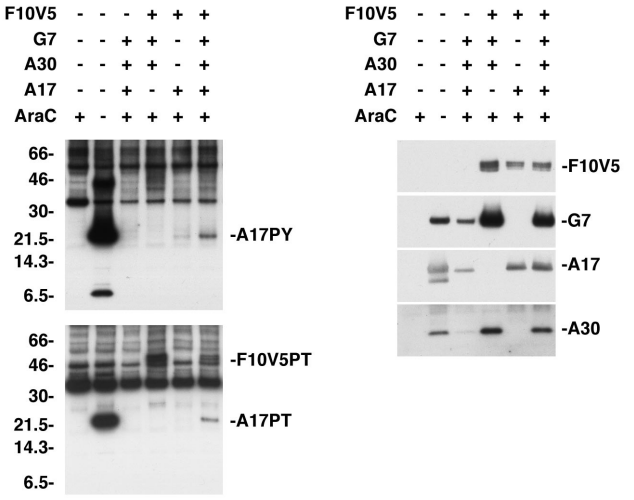

FIG. 7. F10-dependent phosphorylation of A17 was stimulated by A30 and G7 in the absence of other viral late proteins. BS-C-1 cells were infected with vTF7-3 in the presence (+) or absence (−) of AraC and either not transfected (−) or transfected (+) with combinations of plasmids containing the F10V5, G7L, A30L, or A17L ORF regulated by a bacteriophage T7 promoter. Twenty-four hours after infection, the cells were harvested and whole-cell lysates were analyzed by electrophoresis in an SDS–10 to 20% polyacrylamide gel in Tricine buffer followed by Western blotting with anti-pTyr or anti-pThr antibodies. The bands corresponding to the A17 and F10V5 proteins recognized by the anti-pTyr (A17PY) and anti-pThr (A17PT and F10V5PT) antibodies are indicated on the right. The membranes were stripped and reprobed with antibodies against F10V5, G7, A17, and A30, as indicated on the right. The migration positions and molecular masses of marker proteins, in kilodaltons, are indicated on the left.

portion of a blot probed with antibody against F10. The intensity of the band detected with lysates of cells infected with the F10 inducible virus in the presence of IPTG, but not in its absence, documented the specificity of the antibody. Remarkably, the F10 band was not detected from cells infected with vA30Li or vG7Li in the absence of IPTG. Inhibition of A9 or A17 expression also decreased the levels of F10, albeit to a lesser extent than in the absence of A30 or G7, indicating that F10 is very sensitive to the status of the infection. The blots were also probed with antibodies against G7 and A30 in order to determine whether F10 expression affected their synthesis or stability. Both A30 and G7 levels were actually increased when F10 expression was repressed in the absence of IPTG, but they were unaffected by repression of A9 or A17 (Fig. 6, rows 2 and 3). As we previously reported, the stabilities of A30 and G7 were dependent on each other. The inability to pulse-label F10 even in the presence of IPTG, presumably because the protein is synthesized in small amounts, precluded quantification of its stability.

We also examined the expression and phosphorylation of A17 under the above conditions using antibodies against pThr and pTyr. The pattern in the absence of F10 expression was very similar to that obtained in the absence of either A30 or G7 (Fig. 6, rows 4 and 5). In each case, tyrosine and threonine phosphorylation of A17 correlated with expression of F10.

G7 and A30 stimulate phosphorylation of A17 in the absence of other viral late proteins. The apparent stabilization of F10 by A30 and G7 could explain why the latter proteins were necessary for kinase activity. We next inquired whether A30 and G7 were sufficient to stimulate F10 kinase activity in the absence of other viral late proteins. Cells were infected with recombinant VV vTF7-3, which expresses the bacteriophage T7 RNA polymerase, in the presence of AraC to prevent viral DNA replication and synthesis of viral late proteins, including F10, A17, A30, and G7. When plasmids containing the F10V5 and the A17L ORFs regulated by the T7 promoter were transfected into cells infected with vTF7.3 in the presence of AraC, only a very faint band corresponding to tyrosine- and threonine-phosphorylated A17 was detected (Fig. 7, left panels). However, when plasmids expressing A30 and G7 were cotransfected with those expressing F10V5 and A17, the tyrosine- and threonine-phosphorylated A17 band increased in intensity, suggesting a direct stimulation of the F10 kinase. The inability of plasmids expressing F10 with point mutations in its catalytic site to stimulate A17 phosphorylation (data not shown) confirmed the requirement for F10 kinase activity. A band with an apparent mass of 50 kDa was also detected by anti-pThr antibody in lysates of cells that had been transfected with plasmids expressing F10V5, G7, and A30 (Fig. 7, lower left panel). This 50-kDa band comigrated with F10V5, consistent with the stimulation of F10 kinase autophosphorylation by A30 and G7 shown in Fig. 5B.

We concluded that the stimulation of A17 phosphorylation by A30 and G7 might be due to enhanced stability of either A17 or F10. For determination of their levels of expression, the membranes from the above experiment were stripped and reprobed with anti-V5 antibody or with antibody against G7, A30, or A17. The amount of A17 did not correlate with the expression of G7 or A30 and the amount of F10V5 was only

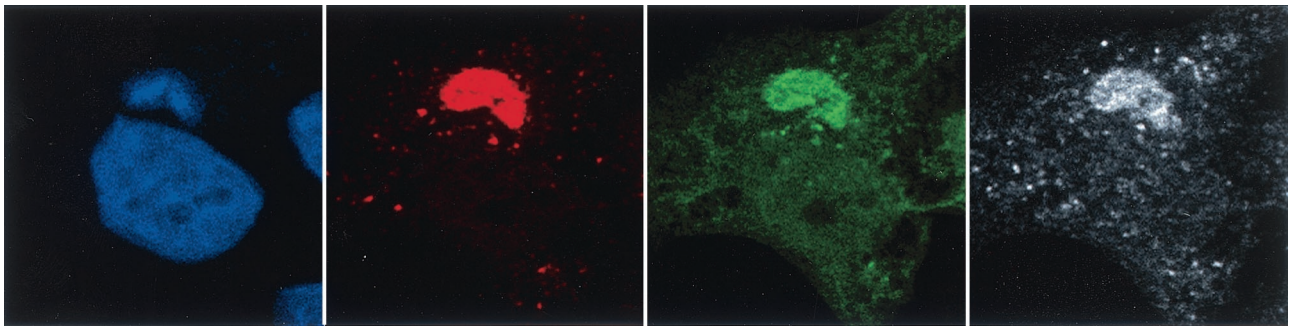

FIG. 8. Localization of F10V5, A30HA, and G7 by confocal microscopy. HeLa cells were infected with vA30iHA-F10V5 in the presence of 25 μM IPTG. At 18 h, cells were fixed, permeabilized, and stained with (i) anti-V5 antibody followed by rhodamine red X-conjugated goat anti-mouse antibody, (ii) anti-G7 antiserum followed by Cy5-conjugated goat anti-rabbit antibody, and (iii) anti-HA antibody directly conjugated to Alexa Fluor 488. Nuclei and viral factories were stained with DAPI and the cells were examined by confocal microscopy. Colors: green, anti-HA; white, anti-G7; red, anti-V5; and blue, DAPI.

slightly reduced in the absence of the two proteins (Fig. 7, right panel). The latter result suggested that the stimulation of kinase activity by A30 and G7 was not solely due to enhancement of F10 stability and also that other viral late proteins must contribute to the instability of F10 in the absence of A30 and G7 when AraC is not present (Fig. 6). In addition, the G7 and A30 bands were most intense when F10 kinase was expressed (Fig. 7, right panel), which was not the case in the absence of AraC (Fig. 6). It should not be too surprising that the expression of three viral late proteins does not accurately mimic the protein dynamics occurring during a normal infection.

F10 is concentrated with G7 and A30 in viral factories. We determined the intracellular locations of F10, A30, and G7 to see if these sites were consistent with their physical interactions. In order to visualize all three proteins simultaneously, cells infected with vA30iHA-F10V5 in the presence of IPTG were stained with a mouse MAb against V5 followed by an anti-mouse antibody conjugated to rhodamine red X, a mouse MAb against HA that was directly conjugated to Alexa Fluor 488, and rabbit polyclonal antibody against G7 followed by anti-rabbit antibody conjugated to Cy5. No significant background was observed with any of the antibodies in uninfected cells and control experiments with the secondary antibodies showed no cross-reactivity between the different species (data not shown). In cells infected with vA30iHA-F10V5, the signals corresponding to F10V5, G7, and A30HA were concentrated in the virus factories, which stained with DAPI, although some additional cytoplasmic staining was detected (Fig. 8). The overlapping of the signals for the three proteins confirmed the proximity of F10, G7, and A30 during VV infection.

Localization of F10 in mature and immature virus particles. The location of virion-associated proteins is usually determined by extraction with a nonionic detergent and reducing agent. Typical membrane proteins are extracted, whereas core proteins remain insoluble. Some proteins, however, are partially extracted, suggesting a location between the core and membrane. Our previous studies indicated that A30 was in the latter category but that G7 behaved as a typical core protein (13, 16). Although the F10 kinase was originally isolated from virus cores (8), the distribution of the protein in the core and membrane fractions was not determined. We treated sucrose gradient-purified virions with the nonionic detergent NP-40, with or without dithiothreitol, and centrifuged the suspension in order to separate the detergent-soluble proteins from the insoluble core fraction. Analysis of samples by SDS-PAGE and immunoblotting using F10 antiserum revealed that the kinase was exclusively associated with the insoluble core fraction (Fig. 9). As a control, the nitrocellulose membrane was stripped and reprobed with an antibody against the A14 membrane component; the control was completely solubilized with NP-40 and dithiothreitol (Fig. 9).

Immunoelectron microscopy was also used to determine the localization of F10. Cell monolayers were infected with vF10V5i in the presence or absence of IPTG and subsequently stained with V5 MAb followed by protein A conjugated to gold spheres. No gold particles were associated with viral structures in cells infected in the absence of IPTG, indicating the absence of a significant background (not shown). In the presence of IPTG, gold particles were seen in association with immature virions; the majority of the label was in the cortical region, close to the concave surface of the viral membrane (Fig. 10A and B). Gold particles were found in a corresponding location within mature virions (Fig. 10C), although they were less abun-

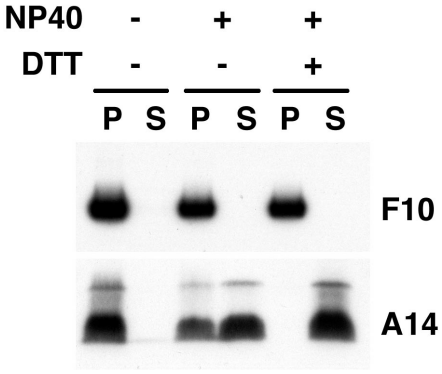

FIG. 9. Localization of F10 by biochemical fractionation of purified virions. Sucrose gradient-purified VV was incubated in Tris buffer containing 1% NP-40, with or without 50 mM dithiothreitol, and then centrifuged to separate the detergent-soluble membrane (S) and insoluble core (P) fractions. Proteins were analyzed by SDS-PAGE followed by Western blotting using anti-F10 or anti-A14 antiserum as indicated.

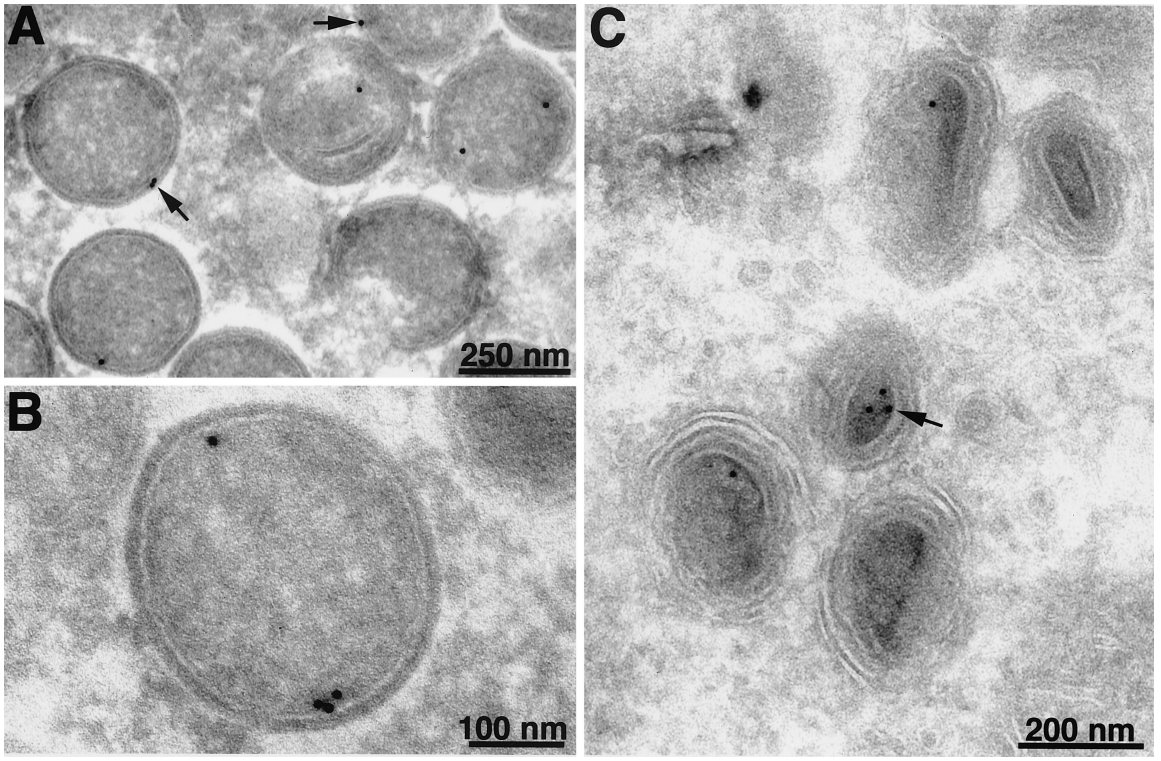

FIG. 10. Localization of F10V5 by immunoelectron microscopy. BS-C-1 cells were infected with vF10V5i at a multiplicity of infection of 10 in the presence of 50 μM IPTG. Twenty-two hours after infection, the cells were fixed in paraformaldehyde, cryosectioned, and incubated with anti-V5 MAb followed by rabbit anti-mouse IgG and protein A conjugated to colloidal gold. Arrows point to representative gold grains. Electron micrographs are shown with scale bars.

dant than in immature virions, perhaps because of poorer accessibility to the antibody.

DISCUSSION

Electron micrographs of VV-infected cells show large cytoplasmic regions from which mitochondria and other cellular organelles are largely excluded. Within these viral factory areas, crescent membranes encompass distinct electron-dense granular masses of viroplasm that are destined to form internal components of infectious virus particles. Although the viroplasm appears amorphous, an underlying network of protein-protein interactions appears to exist. Recently, we identified two viroplasmic proteins, A30 and G7, which interact with each other and are required for the association of the viroplasm with membranes (13, 15, 16). We speculated that through additional protein-protein interactions, A30 and G7 link the viroplasm with the membrane. A clue to such a link was obtained in the present study when we noted that the A17 integral membrane component remained unphosphorylated by the F10 kinase in the absence of A30 or G7. We first thought that the block in phosphorylation was simply due to the spatial separation of the viroplasm and crescent membranes. To our surprise, we uncovered a physical interaction between A30, G7, and F10.

Direct evidence for an A30-G7-F10 complex came from the coimmunoprecipitation of the three proteins from a lysate of infected cells. Coimmunoprecipitation occurred with antibody against either F10 or A30. The findings that A30 undergoes F10-dependent phosphorylation and that autophosphorylation of F10 is stimulated by A30 provided additional evidence of interactions between these proteins. Nevertheless, the complex formed even with mutated catalytically inactive F10. Moreover, just as A30 and G7 are dependent on each other for stability, we found that F10 was nearly undetectable in the absence of A30 and G7. The reverse was not true, however, as repression of F10 did not diminish the amounts of A30 and G7. F10 is not an abundant protein and our inability to adequately pulse-label it, even during a normal infection, precluded quantitative measurements of F10 degradation. Other explanations for the dependence of F10 on A30 and G7, such as regulation of synthesis, seem unlikely. The instability of F10, however, appears complex, since F10 was stable when expressed by transfection in the absence of other viral late proteins and was diminished under certain other nonpermissive conditions of infection.

The present studies and those in our companion paper (14) fill in some previous gaps in the characterization of F10. Like A30 and G7, F10 is expressed late in infection and is concentrated in the factory regions. Immunoelectron microscopy suggested that F10 is present in the cortical region of immature virions, beneath the outer membrane where A17 is located. A corresponding location in mature virions was suggested, although gold grains were less abundant there, possibly due to antibody inaccessibility. Biochemical experiments also indicated that F10 was located in the particulate core fraction of mature virions. In previous experiments, A30 and G7 were

found to be associated with the core fraction, although A30 was partially released by treatment with a detergent and reducing agent (13, 16).

The number of proteins in the A30-G7-F10 complex is still under investigation. Recently, Chiu and Chang (2) discovered that repression of J1 gave a phenotype similar to that found when A30 or G7 was repressed. Immunoprecipitation with antibody against either A30 or F10 indicated that J1 is also associated with the complex, and preliminary data suggest that there are additional interacting proteins (P.S., unpublished data). Further studies will be needed to define the precise protein-protein interactions within this growing complex. Nevertheless, direct interaction between F10 and A30 or G7 is suggested by the phosphorylation of A30 and the ability of A30 and G7 to stimulate A17 phosphorylation in the absence of other viral late proteins.

Approximately 100 viral proteins are expressed late in infection and many, if not most, of these seem to be incorporated into virus particles. The formation of protein complexes such as the one involving A30 and another comprised of proteins involved in the transcription of early genes (23) may facilitate the ordered assembly of the virion components.

ACKNOWLEDGMENTS

We thank the members of the Laboratory of Viral Diseases for their interest and suggestions, in particular Brian Ward for assistance with confocal microscopy and Norman Cooper for the tissue culture cells.

REFERENCES

1. **Betakova, T., E. J. Wolffe, and B. Moss.** 1999. Regulation of vaccinia virus morphogenesis: phosphorylation of the A14L and A17L membrane proteins and C-terminal truncation of the A17L protein are dependent on the F10L protein kinase. J. Virol. **73:**3534–3543.
2. **Chiu, W. L., and W. Chang.** 2002. Vaccinia virus J1R protein: a viral membrane protein that is essential for virion morphogenesis. J. Virol. **76:**9575–9587.
3. **Derrien, M., A. Punjabi, R. Khanna, O. Grubisha, and P. Traktman.** 1999. Tyrosine phosphorylation of A17 during vaccinia virus infection: involvement of the H1 phosphatase and the F10 kinase. J. Virol. **73:**7287–7296.
4. **Earl, P. L., N. Cooper, S. Wyatt, B. Moss, and M. W. Carroll.** 1998. Preparation of cell cultures and vaccinia virus stocks, p. 16.16.1–16.16.3. *In* F. M. Ausubel, R. Brent, R. E. Kingston, D. D. Moore, J. G. Seidman, J. A. Smith, and K. Struhl (ed.), Current protocols in molecular biology, vol. 2. John Wiley and Sons, New York, N.Y.
5. **Earl, P. L., and B. Moss.** 1998. Characterization of recombinant vaccinia viruses and their products, p. 16.18.1–16.18.11. *In* F. M. Ausubel, R. Brent, R. E. Kingston, D. D. Moore, J. G. Seidman, J. A. Smith, and K. Struhl (ed.), Current protocols in molecular biology, vol. 2. John Wiley and Sons, New York, N.Y.
6. **Fuerst, T. R., E. G. Niles, F. W. Studier, and B. Moss.** 1986. Eukaryotic transient-expression system based on recombinant vaccinia virus that synthesizes bacteriophage T7 RNA polymerase. Proc. Natl. Acad. Sci. USA **83:**8122–8126.
7. **Guan, K., S. S. Broyles, and J. E. Dixon.** 1991. A Tyr/Ser protein phosphatase encoded by vaccinia virus. Nature **350:**359–362.
8. **Lin, S., and S. S. Broyles.** 1994. Vaccinia protein kinase 2: a second essential serine/threonine protein kinase encoded by vaccinia virus. Proc. Natl. Acad. Sci. USA **91:**7653–7657.
9. **Liu, K., B. Lemon, and P. Traktman.** 1995. The dual-specificity phosphatase encoded by vaccinia virus, VH1, is essential for viral transcription in vivo and in vitro. J. Virol. **69:**7823–7834.
10. **Rodriguez, D., J. R. Rodriguez, and M. Esteban.** 1993. The vaccinia virus 14-kilodalton fusion protein forms a stable complex with the processed protein encoded by the vaccinia virus A17L gene. J. Virol. **67:**3435–3440.
11. **Rodriguez, J. R., C. Risco, J. L. Carrascosa, M. Esteban, and D. Rodriguez.** 1997. Characterization of early stages in vaccinia virus membrane biogenesis: implications of the 21-kilodalton protein and a newly identified 15-kilodalton envelope protein. J. Virol. **71:**1821–1833.
12. **Rodriguez, J. R., C. Risco, J. L. Carrascosa, M. Esteban, and D. Rodriguez.** 1998. Vaccinia virus 15-kilodalton (A14L) protein is essential for assembly and attachment of viral crescents to virosomes. J. Virol. **72:**1287–1296.
13. **Szajner, P., H. Jaffe, A. S. Weisberg, and B. Moss.** 2003. Vaccinia virus G7L protein interacts with the A30L protein and is required for association of viral membranes with dense viroplasm to form immature virions. J. Virol. **77:**3418–3429.
14. **Szajner, P., A. S. Weisberg, and B. Moss.** 2004. Evidence for an essential catalytic role of the F10 protein kinase in vaccinia virus morphogenesis. J. Virol. **78:**257–265.
15. **Szajner, P., A. S. Weisberg, and B. Moss.** 2001. Unique temperature-sensitive defect in vaccinia virus morphogenesis maps to a single nucleotide substitution in the A30L gene. J. Virol. **75:**11222–11226.
16. **Szajner, P., A. S. Weisberg, E. J. Wolffe, and B. Moss.** 2001. Vaccinia virus A30L protein is required for association of viral membranes with dense viroplasm to form immature virions. J. Virol. **75:**5752–5761.
17. **Takahashi, T., M. Oie, and Y. Ichihashi.** 1994. N-terminal amino acid sequences of vaccinia virus structural proteins. Virology **202:**844–852.
18. **Traktman, P., A. Caligiuri, S. A. Jesty, and U. Sankar.** 1995. Temperature-sensitive mutants with lesions in the vaccinia virus F10 kinase undergo arrest at the earliest stage of morphogenesis. J. Virol. **69:**6581–6587.
19. **Traktman, P., K. Liu, J. DeMasi, R. Rollins, S. Jesty, and B. Unger.** 2000. Elucidating the essential role of the A14 phosphoprotein in vaccinia virus morphogenesis: construction and characterization of a tetracycline-inducible recombinant. J. Virol. **74:**3682–3695.
20. **Wang, S., and S. Shuman.** 1995. Vaccinia virus morphogenesis is blocked by temperature-sensitive mutations in the F10 gene, which encodes protein kinase 2. J. Virol. **69:**6376–6388.
21. **Wolffe, E. J., D. M. Moore, P. J. Peters, and B. Moss.** 1996. Vaccinia virus A17L open reading frame encodes an essential component of nascent viral membranes that is required to initiate morphogenesis. J. Virol. **70:**2797–2808.
22. **Yeh, W. W., B. Moss, and E. J. Wolffe.** 2000. The vaccinia virus A9 gene encodes a membrane protein required for an early step in virion morphogenesis. J. Virol. **74:**9701–9711.
23. **Zhang, Y., B.-Y. Ahn, and B. Moss.** 1994. Targeting of a multicomponent transcription apparatus into assembling vaccinia virus particles requires RAP94, an RNA polymerase-associated protein. J. Virol. **68:**1360–1370.